

TESTING THE EVOLUTIONARY LINK BETWEEN TYPE 1 AND TYPE 2 QUASARS WITH MEASUREMENTS OF THE INTERSTELLAR MEDIUM

Jinyi Shangguan and Luis C. Ho (arXiv:1902.02377)

In a popular scenario for the coevolution of massive black holes and galaxies, major mergers of gas-rich galaxies fuel vigorous star formation and obscured (type 2) quasar activity until energy feedback from the active galactic nucleus clears away the gas and dust to reveal an unobscured (type 1) quasar. Under this scenario, the precursor type 2 quasars should be more gas-rich than their type 1 counterparts, and both types of quasars are expected to be gas-deficient relative to normal, star-forming galaxies of similar stellar mass. We test this evolutionary hypothesis by investigating the infrared ($\sim 1 - 500 \mu\text{m}$) spectral energy distribution of 86 optically selected $z < 0.5$ type 2 quasars, matched in redshift and [OIII] luminosity to a comparison sample of type 1 quasars. Contrary to expectations, the gas content of the host galaxies of type 2 quasars is nearly indistinguishable from that of type 1 quasar hosts, and neither type exhibits the predicted deficit in gas relative to normal galaxies. The gas mass fraction of quasar hosts appears unaffected by the bolometric luminosity of the active nucleus, although their interstellar radiation field is preferentially higher than that of normal galaxies, potentially implicating active galactic nucleus heating of the large-scale galactic dust.

starburst → major merger → QSO2 → QSO1の進化過程を検証
 ⇒ gas量で QSO1 < QSO2 < normal, star-forming となるはず

Shangguan+ 2018での $z < 0.5$ の Palomar-Green QSO1 と赤方偏移と [OIII] 光度が一致する QSO2 について complete IR SED の fitting
 ⇒ dust mass から gas mass
 ⇒ 予想と反する結果。ガスの性質はほぼ一緒。
 ⇒ viewing angle?

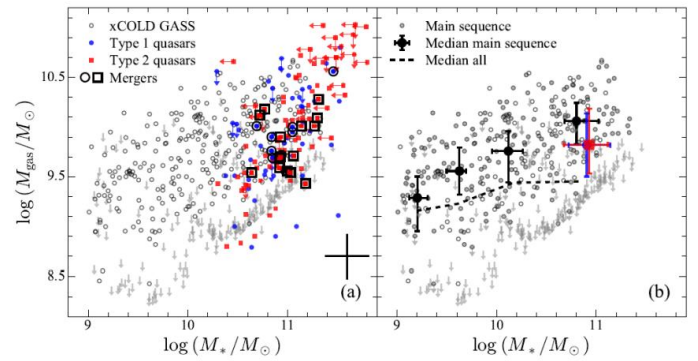


Figure 4. The gas and stellar masses of quasars compared to those normal galaxies. The individual objects are plotted in (a), while the medians of the quasars and normal galaxies are shown in (b). Type 2 quasars (red squares) display similar distributions of M_{gas} and M_* as type 1 quasars (blue circles), and both quasar types resemble star-forming galaxies (grey circles). Median gas and stellar masses of the two quasar types are very similar. They are also consistent with those of the normal galaxies on the main sequence (individual objects: filled grey circles; median: large black circles). The possible differences between the median gas mass and stellar mass of quasars and main-sequence galaxies in the most massive bin are well within the error bars. Meanwhile, quasars show higher gas masses compared to the median of all the normal galaxies (dashed line), as many gas-poor galaxies are included. Quasars at $z < 0.15$ involved in a galaxy merger [large empty circles and squares in (a)] do not stand out in any particular way. The error bars in (a) illustrate the typical uncertainty of the gas and stellar masses for the quasars. The error bars in (b) represent the 25th-75th percentile ranges of the sample distribution.

⇒ QSO1, QSO2 で違いはなく MS とも区別つかない
 merger 的な形態のものも他に埋もれている

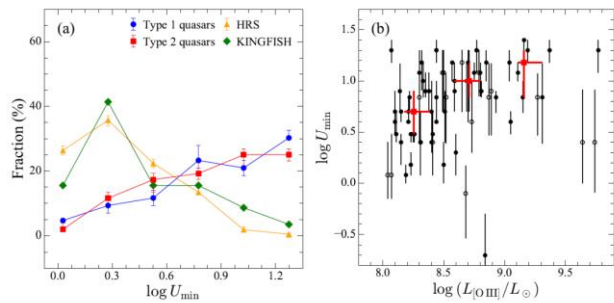
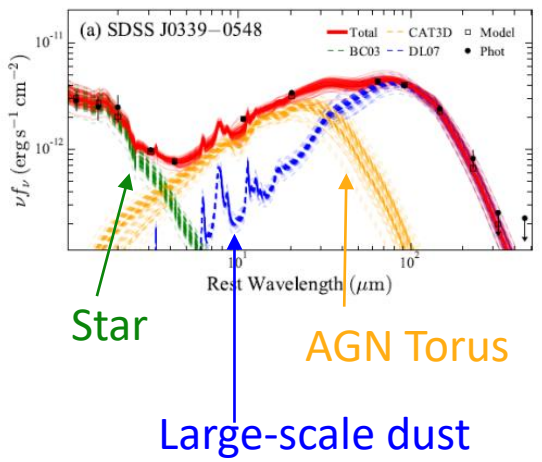


Figure 3. The dust-probed interstellar radiation field. (a) Distribution of U_{min} for type 1 quasars (blue circles), type 2 quasars (red squares), and normal galaxies from the KINGFISH (green diamonds) and HRS (orange triangles) samples. The errors for the quasars and HRS galaxies are estimated with a Monte Carlo method, resampling the parameters according to their measured errors and calculating the number of galaxies in each bin for 500 times. The error bars represent 25th-75th percentile ranges of the resampled distribution in each bin. Since measurement errors of the KINGFISH galaxies are not available, no error bars are associated with the green diamonds. The star-forming and quenched galaxies in the KINGFISH and HRS samples peak at low U_{min} . By contrast, the host galaxies of both types of quasars tend to have higher U_{min} . (b) The values of U_{min} for type 2 quasars generally increase with increasing [OIII] luminosity. The filled circles represent more robust measurements than the open circles; we omitted objects for which only upper limits are available for the dust mass. To better visualize the observational trend, we grouped the sample into three bins: $\log L_{\text{OIII}} < 8.5$, $8.5 - 9.0$, and ≥ 9.0 ; the 50th percentile of the distribution in each bin is plotted as red squares with error bars.

U_{min} が同じ ⇒ dust 分布が類似 ⇒ concentration
 $L[\text{OIII}]$ と相関 ⇒ AGN は銀河の広い範囲に影響

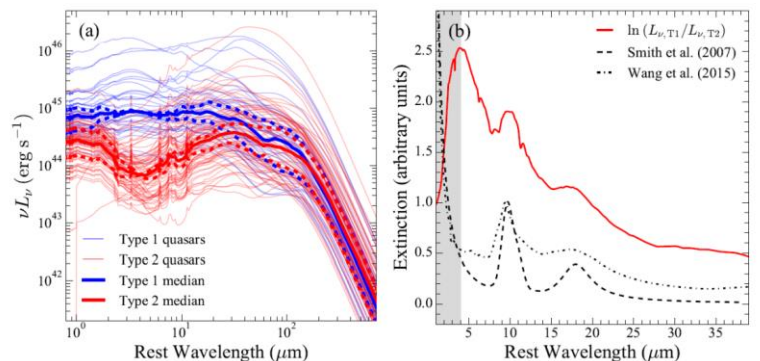


Figure 5. Comparison of median SEDs. (a) The median curves of type 1 (solid blue curve) and type 2 (solid red curve) quasars are calculated from the median of the best-fit models (thin lines) normalized at $4 \mu\text{m}$ and scaled to the median luminosities of the normalization at $4 \mu\text{m}$. The 25th-75th percentile spread of the distribution is shown as dotted lines. Type 1 quasars are significantly brighter than type 2 quasars up to $\sim 40 \mu\text{m}$. At longer wavelengths, the two types have roughly similar SEDs. (b) The ratio of the median SEDs for type 1 and type 2 quasars (red curve), which reflects the extinction if the difference between the two median SEDs is due solely to optically thin dust extinction. The ratio drops below $\sim 4 \mu\text{m}$ (shaded region) because stellar emission dominates the near-IR SED. The overall rise below $35 \mu\text{m}$ and the bumps at ~ 10 and $18 \mu\text{m}$ are features of the Milky Way extinction curve (e.g., dashed line and dot-dashed line).

FIR の SED は一致 ⇒ dust content が類似
 MIR の SED は QSO2 が obscure な分だけ違う